

3.1 Polarization Behavior of Active Passive Metals and Alloys

John R. Scully, Katie Lutton

Center for Electrochemical Science and Engineering

Department of Materials Science and Engineering

University of Virginia, Charlottesville, VA, United States

Glossary

Symbol	Explanation
E_p	Primary passivation potential
E_{P2}	Primary activation potential
i_{crit}	Critical current density
E_{trans}	Transpassive potential
E_{P1}	First primary passivation potential
E_p^0	Hypothetical standard primary passivation potential based on a half-cell reaction
τ_p	Critical time for passivation
SHE	Standard hydrogen electrode
i_{pass}	Passive current density
i_{lim}	Limiting current density for a mass transport limited cathodic reaction

Abstract

The objective of this chapter is to summarize the relationships between electrochemical potential and current density for typical transition metals such as Fe, Cr, and Ni. Key parameters such as the active passive transition, primary and secondary passivation potentials, critical anodic current density, passive current density, and transpassive region are presented, defined, and interpreted to explain typical E-log(i) diagrams and polarization curves. Consideration is given to the polarization behavior of a passivating electrode resulting from both the anodic and cathodic partial currents using mixed potential theory. The impact of the reversible electrode potential and polarizability of an oxidizing reducible species on the observed E-log(i) polarization behavior of such passivated materials is discussed. The kinetics of the passive film growth on base metals such as Fe, Ni, and Cr are discussed in an accompanying chapter.

Key words: active passive transition, primary and secondary passivation potentials, the critical anodic current density, passive current density, transpassive transition

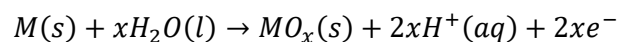
1. Introduction

The thermodynamic stabilities of electrochemically grown oxides on metals can be described by their Pourbaix diagrams [1,2] which present phase equilibria with respect to electrode potential and solution pH (hydrogen ion activity) for a given set of half-cell and chemical reactions. This atlas of

potential–pH diagrams [1] offer a visual representation of the thermodynamic oxidizing and reducing capabilities of the major stable oxides, hydroxides, and oxyhydroxides of a and are used frequently in electrochemical applications to understand the effects of electrochemical potential and pH on the phase stability of chemical compounds. These diagrams are determined from standard Gibbs free energies of formation of the oxides or hydroxides considered, ΔG_f , following thermodynamic equilibrium relationships (including Nernst equations, with a given aqueous-ion concentration) over the interested ranges of electrode potential and solution pH. The diagrams are often considered over a range of activities for the dissolved species considered. Hereafter the term ‘film’ and/or ‘oxide’ are used for brevity, but it should be recognized that passivating films can consist of oxides, hydroxides, carbonates, phosphates, or have other molecular identities depending on thermodynamic stability. They can also deviate from predictions of thermodynamics of bulk oxides based on metastability and pseudo- or polymorphic effects, possibly influenced by epitaxy, surface energy, interfacial and bulk stresses, or kinetic factors such as fast formation and slow chemical dissolution.

The stable passive region of a metal or alloy is suggested by E-pH diagrams, but the kinetics associated with the anodic reactions as a function of potential are based on a variety of thermodynamic and kinetic factors including the kinetics of oxide formation compared to chemical dissolution, point defect types, ionic and electronic transport characteristics of the oxide in response to the electric field imposed across the oxide and interfacial reaction fluxes (Section 3.2), oxide film solubility, and a number of other factors. The concept of passivity is satisfied if (a) a high corrosion rate is expected under the conditions of exposure without a passive layer, (b) if instead, the corrosion occurs slowly due to either a adsorbate or a thin and dense film of several or more monolayers [3].

The conditions described in (a) can also occur in the presence of strongly adsorbed species such as O_2 , OH^- , or some other adsorbed anionic species that interfere with metal oxidation. On the other hand, there is strong evidence of mono-molecular coverage at the onset of passivity by either O_2 or OH^- compared to H_2O . In general, oxides may be regarded to form via a number of pathways. Direct film formation occurs by reaction of the metal, M, with water to form an adsorbed oxygen layer or compact oxide, MO_x .



In contrast, dissolution-precipitation may occur in a multi-step process where the metal is first oxidized to form cations in solution which then chemically react by precipitation to form an insoluble oxide or other molecular species. This multi-step process may also occur electrochemically such as when anodic deposition of metal cations in solution occurs in sequence after an initial oxidation step. In this case, metal cations are oxidized to a higher valence state to form an insoluble oxide whose oxidation state is higher than the original soluble metal ions. However, it is regarded that in most cases, thin film passivating materials form oxides by spatially homogeneous direct cation ejection, enabling formation of a conformal oxide as opposed to one formed by dissolution-precipitation processes where precipitates may attach to the metal surface with variable coverage and interfacial strengths. In the case of direct reaction with water to form a solid-state oxide, anodic behavior is not dependent on solution stirring.

Protective oxides may be on the scale of nanometers thin and electronically conducting such as for Fe, Ni, and Cr, thicker and insulating such as on Al, Ta, and Zr, or micrometer scale, porous, and often visible such as in the case of Zn, Cd, Mg, and Cu. In each case, the conditions of (a) and (b) may be satisfied even though the circumstances, physical situation, and molecular scale details differ

substantially. In the case of Al, Ta, and Zr, neither transpassivity or oxygen evolution can occur readily due to restricted electronic conductivities and large voltages can be applied without water oxidation to form thick anodized layers. For thin film passivation with a full-coverage nanometer-scaled thin film, the rates of the processes described above and subsequent E-log(i) behavior observed depends on the Galvani potentials established across the metal/film, film, and film/solution interfaces. For instance, it is regarded that cation ejection, cation vacancy or interstitial migration, anion vacancy migration, or dissolution of cations at the film/solution interface control the quasi-steady state passive current density as will be discussed in Section 3.2.

2. Anodic Partial Active/Passive Behavior

Fe in acid solutions

Iron in dilute sulphuric acid presents a well-studied example of thin film passivity. The anodic current increases as an exponential function of potential in region A-B until reaching a critical passivating current density, i_{crit} , is reached at a potential, E_{p1} , whereupon a large decrease in current density is observed in an upward scan or potential hold. B, C, and I indicate decreases in the active response. In the vicinity of E_p , Fe^{2+} is dissolved, while at higher potentials, both Fe^{2+} and Fe^{3+} are dissolved.

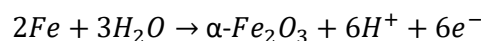
<Figure 1 near here>

E_{p2} is often described as an activation, reactivation, or sometimes a Flade potential. A large range in potential from E_{p2} up to F is observed where iron remains passive and corrodes at a low potential independent rate over this range. The oxide thickens linearly with increasing potential from less than 3 to 5 nm. Such a direct relationship with different absolute values is seen in sodium phosphate and phosphoric acid solutions. The film thickness may be closer to 2-3 nm in acids solutions while greater in more alkaline solutions [4–6]. The origins of the independence between E and i are discussed below, but in short, the film thickens in response to the increased voltage. From F to H, oxygen evolution occurs by the partial anodic reaction: $2H_2O \rightarrow O_2 + 4H^+ + 4e^-$. Transpassivity may also occur as discussed below.

Based on a simplistic assumption, E_p might be regarded as the equilibrium potential of the metal oxide formation reaction which passivates the metal. This is not found to be the case. Consider FeO (wüstite), Fe_3O_4 (magnetite), and $\alpha-Fe_2O_3$ (hematite) formation when Fe reacts with water. Slow hematite dissolution in acid makes this route plausible in acidic solutions [7,8]. None of the equilibrium formation potentials of these oxides compare well with the observed relationship between E_p and pH as experimentally observed at 25°C between pH 0 and 6:

$$E_p^0 (V_{SHE}) = 0.58 - 0.059 \text{ pH}$$

The predicted E_p^0 at pH 0 is still 0.5 V too high. For instance, assuming that the formation of $\alpha-Fe_2O_3$ (hematite) occurs by the following reaction:



yields a predicted Nernst potential expression given as:

$$E_{Fe/\alpha-Fe_2O_3}(V_{SHE}) = -0.05 - 0.059 pH$$

The standard potential for $Fe_3O_4/\alpha-Fe_2O_3$ is somewhat similar to E_p^0 , but electron diffraction suggests a cubic structure [9,10] while in the case of $\alpha-Fe_2O_3$, a rhombohedral corundum structure is believed to exist [11]. However, $\gamma-Fe_2O_3$ can form from Fe_3O_4 as both possess a crystalline cubic spinel lattice and $\gamma-Fe_2O_3$ is supported because it dissolves slowly in acid [12]. Some evidence suggests that the oxide is magnetite with cation vacancies, or $Fe_{3-\alpha}O_4$, which is compatible with $\gamma-Fe_2O_3$ or stoichiometric $Fe_{2.67}O_4$ when $\alpha = 0.33$ [13].

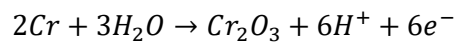
The meaning of the critical current density has also been examined in detail in the case of iron in an acidic solution. The critical current density must be exceeded in order for passivation to occur, but it is also found that a critical time, τ_p , must be exceeded at a given current density (or charge) in order to achieve passivation [14].

$$(i - i_{crit})\tau_p = constant$$

The charge obviously contributes to forming critical conditions for the film, such as a salt layer, which is well-beyond a single monolayer. Ellipsometry supports the view that an oxide of measurable thickness occurs and that direct oxidation occurs as with gas phase oxidation.

Cr in acid solutions

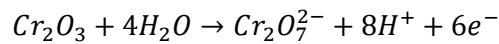
Passivation of chromium in acid follows similar behavior shown in Figure 1 where there is an E_{p1} for passivation and an activation or reactivation potential, E_{p2} . For Cr at a pH of 0.3, E_{p1} is $-0.4 V_{SHE}$ and E_{p2} is $-0.1 V_{SHE}$. The relationship between E_{p2} and pH follows the trend $\frac{dE_{p2}}{d pH} = -0.12 V$ in sulfuric acid [3]. An assumed half-cell reaction might occur as follows:



The passive current density in region DF depends on pH and the exact nature of the species in solution. The anion participating matters as $CrSO_4^+$, $Cr(OH)Cl^+$, and $CrCl^{2+}$ which are often products of chemical dissolution of Cr^{3+} oxides or hydroxides in acid. The passive current density is often lower than for iron e.g. $< 1 \mu A/cm^2$ and independent of potential over a broad potential range of 1 V. i_{crit} is also much smaller than in the case of Fe and the film thickness varies from 1 nm to 2 nm in acid as seen by ellipsometry but varies with potential and pH. In the passive range Cr dissolves as Cr^{3+} ions while the oxide is Cr(III). Cr_2O_3 is often described as the oxide species but the outer layer contains water and is hydrated as in $Cr(OH)_3 \cdot 0.3 H_2O$. Many studies of the oxidation and passivity of pure Cr have been conducted. Room temperature oxidation in oxygen atmospheres and electrochemical passivation leads to the formation of thin, amorphous oxides of partially hydrated Cr_2O_3 . At 300 K a granular, non-crystalline oxide is formed [15–18] up to a limiting thickness of about 0.9 nm [19]. The stoichiometry has been confirmed to be Cr_2O_3 and the oxide becomes increasingly dehydrated to lose the 10-20 at% water as the temperature of the oxygen atmosphere was increases. However, the stoichiometry does not change with thickness nor with temperature. Scanning tunnelling microscopy suggest that initially amorphous Cr_2O_3 subjected to long-term annealing becomes crystalline. However, the crystallinity is accompanied by the annihilation of point defects such as vacancies and interstitials. Hence it is difficult to say whether any improvements with time are due to reduction of defects and crystallization or whether such improvements occur in spite of crystallization. Classically,

crystallization is viewed as detrimental; because of fast path transport of ions (both inward and outward) along grain boundaries.

Transpassive dissolution of Cr occurs at higher applied potential as Cr(VI) oxides, chromate, or dichromate ions are formed in alkaline solution by direct oxidation of Cr_2O_3 such as by the following pathway.



OER does not occur as the current density rises steeply with potential. The film can consist of Cr in various valence states ranging from 2 to 6. The transpassive potential is strongly dependent on solution pH which relates to the half-cell potential pH dependency. The reaction is sluggish as transpassive currents become large at about 1 V_{SHE} which is well above the thermodynamically derived transpassive half-cell potentials

Ni in acid solutions

Ni is passivated in acids by first forming a non-passivating primary layer of NiO. E_{P1} in acid may correspond with the equilibrium potential $E_{\text{Ni}^{2+}}/E_{\text{Ni}_3\text{O}_4}$ or $E_{\text{NiO}}/E_{\text{Ni}_3\text{O}_4}$ [20]. However, as in the case of iron, E_{P1} does not correspond with any single equilibrium potential for Ni oxidation to an oxide or hydroxide. The i_{crit} value critically depends on pH. The i_{pass} value is high at very low pH's such as 0.3, low at pH 5, and rises again at pH 10. It should be noted that there is considerable dynamic or unsteady state passivity owing to fast oxide growth along with chemical dissolution at low pH, while the trend at high pH suggests uncertainty in E-pH thermodynamics associated with oxide stability as discussed elsewhere [21]. The region D-E of Figure 1 is often observed with i_{pass} as low as 10^{-8} A/cm². Passivation of Ni results in formation of $\text{Ni}(\text{OH})_2$, NiO and Ni_3O_4 [20]. Rising passive current density corresponds to release and detection of divalent ions. It has also been attributed to recrystallization of amorphous dense Ni(II) oxide first formed at lower potentials. In boric acid/borate buffer there is steady linear rise in the film thickness with potential at pH 8.52 [20,22]. The likely reaction is:



In region E-F, a second current plateau is likely associated with secondary passivity transpassivity but transpassivity remains unclear and could correspond with a variety of reactions and include Ni oxide in higher oxidation states such as NiOOH and Ni_2O_3 [20]. High polarization results in crystalline NiOOH formation and some secondary passivity albeit at much high passive current densities. Increasing current at high potentials has been attributed to release of Ni^{3+} [5]. It seems that crystallization of Ni-oxides is detrimental and associated with current increases. However, in contrast it is unclear whether crystallization of Cr_2O_3 is detrimental (as discussed above). As an oxide grows it is constrained to the metallic surface and may develop both compressive and tensile stresses. If an oxide were to develop sufficient stresses in order to spall or crack at very long exposure times then growth could approach some other kinetics such as linear growth (Section 3.2). There is no evidence to date that this is the case.

Alloys in acid solutions

The improvement in passivity through alloying is generally regarded as due to lower i_{crit} and E_{P1} . In general, both of these parameters are reduced with increasing alloying concentration in solid

solution such that a rate of the cathodic reaction on the passive surface occurs at a greater rate than i_{crit} and E_{P1} .

<Figure 2 near here>

Figure 2 illustrates the case where i_{crit} is lowered along A-B-C-D with alloying content. When the concentration of the alloying element reaches a certain level, spontaneous passivation can occur. The i_{pass} above E_{P2} is often reduced as well. Often the alloying element is enriched in the passive film and the open circuit potential may shift from E_A or E_B to E_C or E_D which are the coupled or open circuit potentials established between the various anodic partial current densities and the single cathodic partial current density indicated (Section 3.2 below). A critical concentration of alloying elements may or may not be observed but various theories for a critical concentration have been posited including enrichment of for instance Cr in the oxide as a high fraction of all oxidized species as a result of slow migration and selective dissolution of chemical dissolution of a differing solvent alloying element [23]. Graph theory has been proposed to provide a geometric explanation that relates the surface concentration of a beneficial passivating element to the surface concentration needed to form a bridging oxide that covers the surface [2,24,25]. The roles of noble alloying elements such as Pt, Pd, or Cu in Cr, Ni-Cr, Ti alloys is often different. A change in i_{crit} and E_{P1} is often not the effect of the such alloying elements. Instead the effects of these species are to catalyse the cathodic reaction such that the rate of the cathodic reaction is enhanced. Consequentially the OCP is raised above E_{P2} such as given by E_C and E_D .

In Figure 3 the E-log(i) behaviors of Fe, Cr and Fe-Cr solid solution alloy are indicated. As seen, a large i_{crit} and positive E_P observed for Fe are reduced by Cr alloying and absent altogether in high purity Cr where E_{H/H^+} may be above E_{P1} for Cr_2O_3 . In many binary or ternary alloys, the effect of beneficial alloying additions such as Cr is to reduce E_{P1} and i_{crit} proportional to the alloying content added.

<Figure 3 near here>

The effects of Cr and Mo in Fe-base alloys and Ni base alloys are noteworthy. Fe-Cr, Fe-Ni-Cr and Ni-Cr alloys produce the effect on i_{crit} and E_{P2} discussed above. Mo also is impactful even though Mo is not regarded by itself as a passivating element. Mo usually effects i_{crit} significantly by hindering active dissolution but might also effect i_{pass} . The effect of Mo on pitting and crevice corrosion is often substantial but is discussed elsewhere. The exact beneficial effects of Mo on oxides and passivity are uncertain. While Mo is known to be beneficial towards crevice corrosion and pitting in Fe-Cr-Mo and Ni-Cr-Mo alloys, its benefit to passivity is less thoroughly investigated. Some literature proposes that Mo is incorporated into the passive state as Mo(IV) or Mo(VI) species. Macdonald's point defect theory proposes that such oxidized Mo is beneficial towards passivity and pit-type oxide breakdown because it attracts and captures cation vacancies such that detrimental cation vacancy clusters do not form [26,27]. Indeed, Mo(VI) is observed in oxides on 20Cr-25Ni-XMo steels [28]. However, this was only seen in air oxidation and upon anodic polarization. Thus, the effects of Mo on stainless steel passivity is partly unclear because of the uncertainty over whether the open circuit potential is oxidizing enough to enable oxidation of Mo(III) to Mo(VI). Lillard concluded that this is less of an issue for Alloy 625 owing to more positive OCPs [29]. Mo (IV) and Mo(VI) are thought to provide soluble MoO_4^{2-} that

could promote self-healing [29,30], a precipitated compound [29,31] or direct incorporation in passive films [32–34].

Ni-Cr-Mo alloys are dominated by Cr_2O_3 when a certain composition of Cr exists in solid solution. On Ni-rich materials, NiO is often described as a cation-defective oxide containing Ni^{2+} and Ni^{3+} . Ni^{3+} leads to vacancy formation [35]. Therefore, the additions of small amounts of Cr to Ni can actually lead to additional vacancies when isolated Cr^{3+} species is present. Oxidation rate can then actually be enhanced because of formation of additional vacancies. However, when enough Cr is added to form a more-or-less continuous Cr_2O_3 film, instead of substitution of Cr^{3+} in NiO, the oxidation resistance is improved significantly. Ni with 20% Cr is very resistant to oxidation and passive current densities in aqueous solutions are reduced as the Cr equivalent concentration is raised [29]. Therefore, alloys like C-22 and 625 contain enough Cr to obtain this benefit.

3. Polarization Curves of Active-Passive Metals and Alloys in the Presence of a Cathodic Reaction: The Origins of Spontaneous Passivity

The combination of anodic E-log(i) processes on a passive metal and a supporting cathodic reaction on the same surface can develop various open circuit potentials either within the passive range or in the active range, depending upon the reversible electrode potentials and reaction rates or extent of polarization on the slow oxidizing reactions on the film-covered surface. It is well-recognized that electronically conducting oxides on passive metals can support cathodic reduction reactions which often require electron transport through the semiconductor to and electron transfer at the film/solution interface. The anodic and cathodic kinetics must be carefully considered together on the passivating material using an Evans diagram to determine whether the open circuit potential lies in the active, passive, or transpassive potential range. Consider the anodic reactions shown in Figure 4 when balanced by the available cathodic reactions shown on the passive electrode.

<Figure 4 near here>

The cathodic electron transfer reaction is regulated by the electronic conductivity of the film-covered surface and its reactivity or the concentration, stirring rate, and diffusion boundary layer thickness of the oxidizer and/or cathodic reactant. Various cathodic reactions must be considered as in any corrosion cell. These may include water and proton reduction which produce hydrogen evolution in reducing acids or neutral and alkaline solutions. Possible cathodic reactions may also include other oxidizers such as dissolved gaseous species like O_2 as well as acids. In fact, natural passivity was observed by Evans in experimental observations of iron in intermediate concentrations of nitric acid solutions of intermediate concentrations [7,8]. The iron electrode may be passivated by other redox reactions as well such as $\text{Ce}^{4+}/\text{Ce}^{3+}$ and $\text{Fe}^{3+}/\text{Fe}^{2+}$ as well as nitrate, phosphate, and other species [36]. Consider the case shown in Figure 4 with an unidentified cathodic reaction. The series of curves labelled B through F indicate progressively faster cathodic reaction rates. The anodic partial current density is labelled A.

A material is often called 'spontaneously passive' if the open circuit potential for a freely corroding system is above E_{P2} but below the transpassive potentials for fast cathodic kinetics. This situation exists for cathodic reaction at OCP's where i_{pass} is balanced by the prevailing cathodic reaction rate. Of course, to achieve this condition the Nernst potential or E_{redox} of the cathodic half-cell reaction must be well above E_{P2} but the exact details depend on both E_{redox} and the cathodic reaction rate on the passivating metal. For instance, various reversible electrode potentials from E_{redox} to E_3 indicated in Figure 4 may produce an OCP above E_{P2} depending on the potential dependent reaction kinetics as indicated by curves B, C, D, and E. The active region is not observed in an experimental polarization curves, impacting the net current density versus potential behavior especially if fast water or proton reduction reactions occur at potentials above E_{P2} . This situation is observed in the case of Cr or Cr-containing alloys such as Ni-Cr in some strong acids but this is not typically observed for Ni and Fe. Alloys such as Zr, Al, and Ti may or may not be passivated in water in acids and even in neutral or slightly alkaline pH. In the case of Ti, the rate of the cathodic reaction is typically too slow to completely hide the active passive transition unless Ti is alloyed with a noble metal element which catalyses the proton discharge reaction.

In aerated solutions exposed to transition metals, E_{P2} is readily below the reversible electrode potential for the oxygen reduction reaction as shown schematically in Figure 4. The metal or alloy will be spontaneously passive assuming that the oxygen or other oxidizer reduction reactions, such as nitrate in nitric acid, occurs at rate given by D. In all of the situations discussed, an additional required criterion is that the cathodic reduction reaction must be greater than i_{crit} at E_{P1} and E_{P2} or, in general, must occur at a higher cathodic rate than the anodic dissolution kinetics over the potential range from E_{P2} to below E_1 . In fact, iron may be passivated with a number of different species that have a Nernst potential in the passive range and a high exchange current density. These include nitrate, phosphate, cerate, and other species added to solution.

In the case of slow cathodic partial reaction rates given by B or C, the open circuit potential may be in the active range such as given by E_1 or E_2 . A high E_{redox} in the transpassive region may also result in an open circuit potential near transpassive potentials, such as at E_5 . However, such strong oxidizers are rare.

The case of a mass transport limited cathodic reaction is also of interest as shown in Figure 5. Consider the oxygen reduction reaction on a stainless steel or a nickel-based alloy in neutral or alkaline solution. The oxygen reduction reaction may be mass transport limited at i_{lim} given by a controlling reaction rate that is inversely proportional to the diffusion boundary layer thickness. These are shown on curves B, C, D, and E. In this case, several conditions are required for passivity. E_{redox} must be much greater than E_{P2} . However, critically, i_C and i_{lim} must be greater than i_{crit} at E_{P1} . In this case, OCP's such as E_4 are observed. If $i_{lim} < i_{pass}$, the open circuit potential will reside in the active region such as between E_1 and E_3 .

<Figure 5 near here>

It is common to assess anodic partial kinetics in de-aerated environments and without other oxidizers in order to reveal as much of the partial anodic dissolution kinetics as possible without the spontaneous passivation brought about by the presence of strong oxidizers. The anodic polarization

curve is typically developed using potentiostatically applied anodic potentials, causing the electrode reactions to be driven anodically.

4. Summary

The relationships between electrochemical potential and current density for typical transition metals such as Fe, Cr, and Ni were introduced. Key parameters such as the active passive transition, primary and secondary passivation potentials, critical anodic current density, passive current density, and transpassive transitions were interpreted to explain typical E-log(i) partial anodic current - potential diagrams. These key parameters depend critically on potential, the solution species and concentrations, materials, and temperatures among other factors. It is shown that the details of cathodic reactions on passive materials determine whether spontaneous passivity occurs. The growth rates of passive films are discussed in the next chapter.

5. Embedded Tables, Figures, and Captions

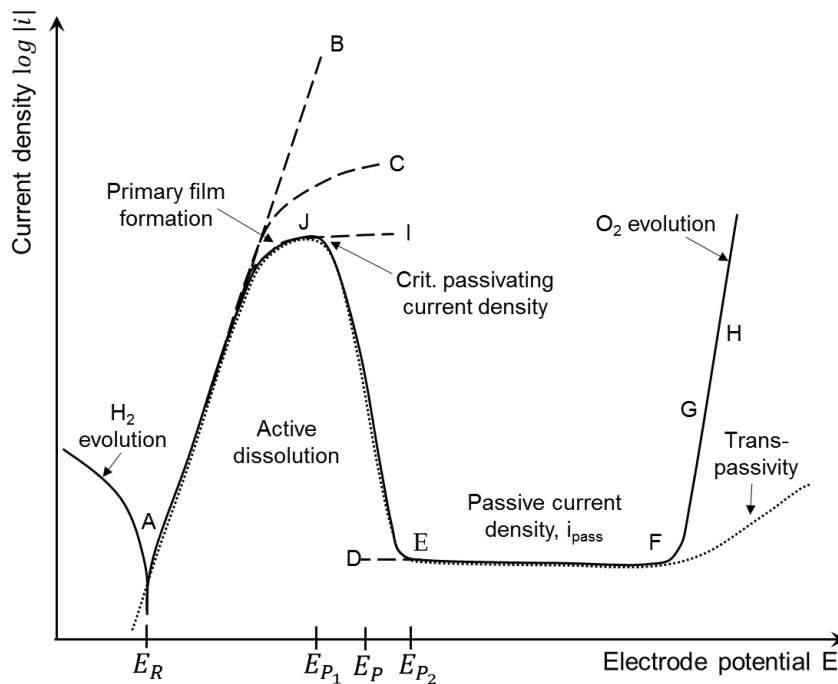


Figure 1. Anodic partial current densities on a metal or alloy I vs. E which contains an active region [A-B], passivity and transpassive behavior. The E-I data from A-B indicates the active charge transfer controlled limit of metal dissolution rate. A critical current density, i_{crit} , is seen at I. The passive range is given from E to F where the passive current density, i_{pass} , is given at D. E_{P1} represents the primary passive potential while E_{P2} represents an activation or reactivation potential. FGH represents the oxygen evolution reaction rate on an electronically conducting or semi-conducting oxide covered metals while transpassivity is observed as represented by the dotted line on some metals. (Redrawn from [3] – approval pending)

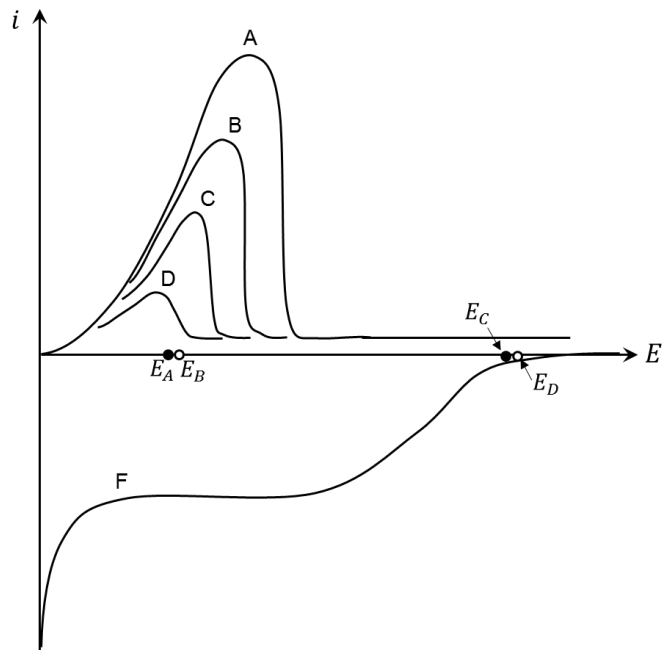


Figure 2. Anodic partial currents indicated by curves A, B, C, and D for increasing alloying content in solid solution. The partial anodic current density for the cathodic reaction is indicated by curve F. (Redrawn from [3] – approval pending)

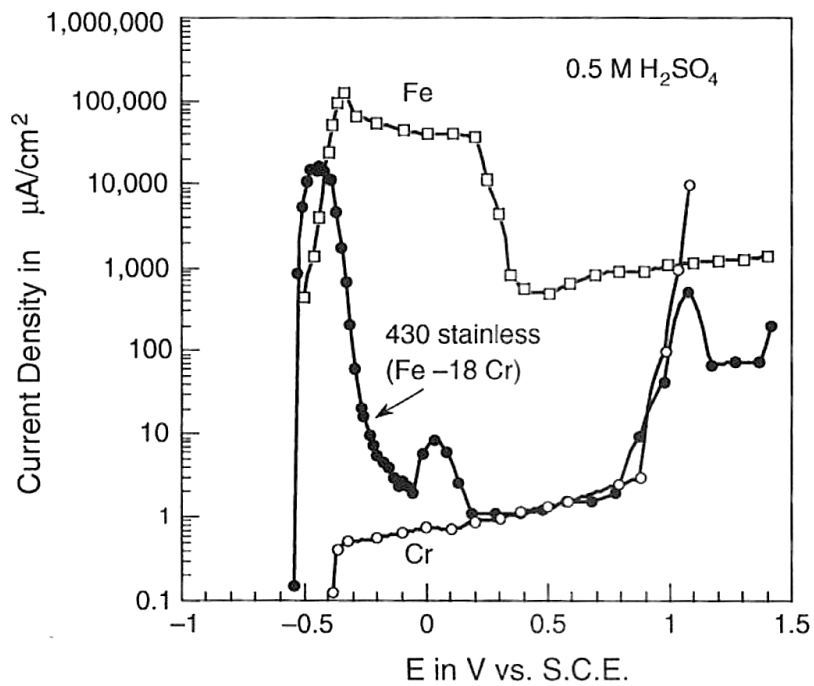


Figure 3. Polarization curves for Cr, Fe, and a solid solution Fe-Cr alloy with 18 wt% Cr in sulphuric acid solution. (– approval pending)

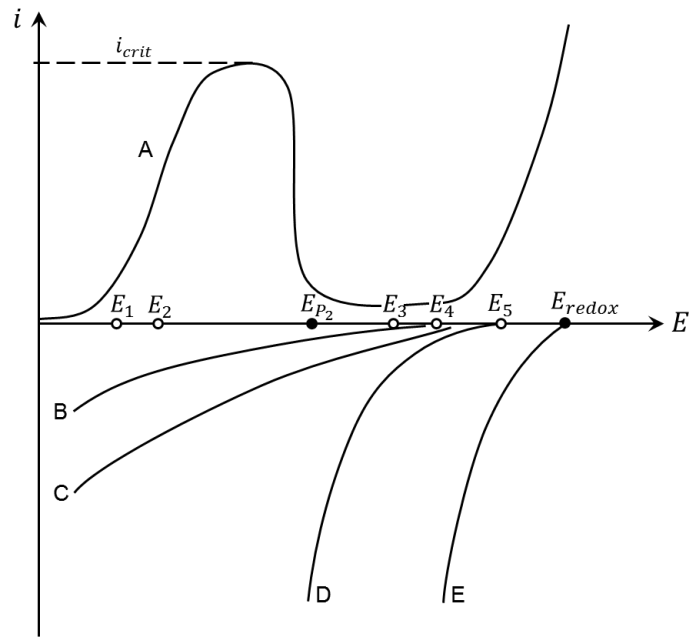


Figure 4. E-I diagram showing anodic and cathodic partial current densities with a range fast and slow cathodic kinetics depicted by curves B through F. Curve A illustrates the anodic partial kinetics. E_{redox} indicates the Nernst potential of the cathodic reaction while i_{crit} is the critical current density. (Redrawn from [3]– approval pending)

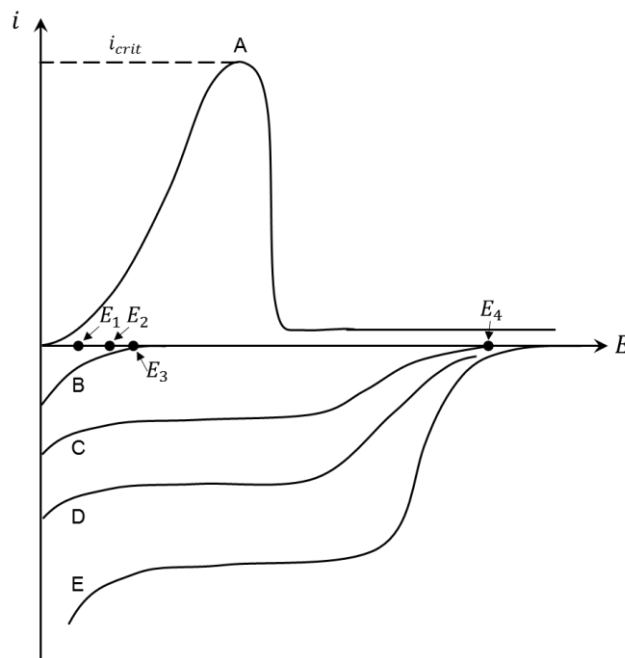


Figure 5. Schematic current-voltage diagram to indicate the strong ennobling of the rest potential upon exceeding a critical electrolyte stirring rate. Curve A indicates the anodic partial kinetics and curves B-E indicate cathodic kinetics with varying mass transport control reaction rates. (Redrawn from [3] – approval pending)

6. References

- [1] M. Pourbaix, Atlas of electrochemical equilibria in aqueous solutions, National Association of Corrosion Engineers, 1974.
- [2] E. McCafferty, Introduction to corrosion science, Springer, 2010. doi:10.1007/978-1-4419-0455-3.
- [3] H. Kaesche, Corrosion of Metals: Physiochemical Principles and Current Problems, 1st ed., Springer-Verlag, Berlin, 2003. doi:10.1007/978-3-642-96038-3.
- [4] N. Sato, M. Cohen, Kinetics of anodic oxidation of iron in neutral solution I. Steady growth region, *J. Electrochem. Soc.* 111 (1964) 512–519. doi:10.1149/1.2426170.
- [5] N. Sato, K. Kudo, An ellipsometric study of anodic passivation of nickel in borate buffer solution, *Electrochim. Acta.* 19 (1974) 461–470. doi:10.1016/0013-4686(74)87025-8.
- [6] N. Sato, T. Noda, K. Kudo, Thickness and structure of passive films on iron in acidic and basic solution, *Electrochim. Acta.* 19 (1974) 471–475. doi:10.1016/0013-4686(74)87026-X.
- [7] M.J. Pryor, U.R. Evans, The Reductive Dissolution of Ferric Oxide in Acid. Part I. The Reductive Dissolution of Oxide Films Present on Iron, *J. Chem. Soc.* (1950) 1259–1266.
- [8] M.J. Pryor, U.R. Evans, The Reductive Dissolution of Ferric Oxide in Acid. Part II. The Reductive Dissolution of Powdered Ferric Oxide, *J. Chem. Soc.* (1950) 1266–1274.
- [9] J. Mayne, J. Menter, The mechanism of inhibition of the corrosion of iron by solutions of sodium phosphate, borate, and carbonate, *J. Chem. Soc.* (1954) 103–107. doi:10.1039/JR9540000103.
- [10] M. Nagayama, M. Cohen, The Anodic Oxidation of Iron in a Neutral Solution, *J. Electrochem. Soc.* 109 (1962) 781–790. doi:10.1149/1.2425555.
- [11] H. Göhr, E. Lange, Der innere elektrische Potentialabfall in der Passivitätsschicht des Eisens und die Flade-Bezugsspannung („Fladepotential“), *Naturwissenschaften.* 43 (1956) 12–13. doi:10.1007/BF00601171.
- [12] E. Lange, H. Weidinger, Aufklärung von Halbzellreaktionen am System Eisen/wässrige Lösung mittels intermittierter Ladekurven, *Naturwissenschaften.* 45 (1958) 383–384.
- [13] C. Wagner, Models for Lattice Defects in Oxide Layers on Passivated Iron and Nickel, *Berichte Der Bunsengesellschaft Für Phys. Chemie.* 77 (1973) 1090–1097. doi:10.1002/BBPC.19730771211.
- [14] U.F. Franck, Elektrochemische Modelle zur saltatorischen Nervenleitung, *Zeitschrift Für Naturforsch. B.* 7 (1952) 220–230.
- [15] S. Ekelund, C. Leygraf, A LEED-AES study of the oxidation of Cr(110) and Cr(100), *Surf. Sci.* 40 (1973) 179–199.
- [16] Y. Sakisaka, H. Kato, M. Onchi, Oxygen chemisorption and initial oxidation of Cr(110), *Surf. Sci.* 120 (1982) 150–170.
- [17] J.S. Foord, Oxygen chemisorption and corrosion on Cr(100) and Cr(110) single crystal surfaces, *Surf. Sci.* 161 (1985) 513–520.
- [18] A.G. Baca, L.E. Klebanoff, M.A. Schulz, E. Paparazzo, D.A. Shirley, Dissociative adsorption of CO and O₂ on Cr(100), Cr(110), and Cr(111) in the temperature range 300–1175 K, *Surf. Sci.* 173 (1986) 215–233.
- [19] V. Maurice, S. Cadot, P. Marcus, XPS, LEED and STM study of thin oxide films formed on Cr(110), *Surf. Sci.* 458 (2000) 195–215. doi:10.1016/S0039-6028(00)00439-8.
- [20] N. Sato, G. Okamoto, Anodic Passivation of Nickel in Sulfuric Acid Solutions Anodic Passivation of Nickel in Sulfuric Acid Solutions, 110 (1963) 605–614. doi:10.1149/1.2425838.
- [21] L.-F. Huang, M.J. Hutchison, R.J. Santucci, J.R. Scully, J.M. Rondinelli, Improved Electrochemical Phase Diagrams from Theory and Experiment: The Ni-Water System and Its Complex Compounds, *J. Phys. Chem. C.* 121 (2017) 9782–9789. doi:10.1021/acs.jpcc.7b02771.
- [22] G. Okamoto, H. Kobayashi, M. Nagayama, N. Sato, Effect of temperature on the passivity of nickel, *Berichte Der Bunsengesellschaft Für Phys. Chemie.* 62 (1958) 775–782.

- [23] R. Kirchheim, B. Heine, H. Fischmeister, S. Hofmann, H. Knote, U. Stolz, The passivity of iron-chromium alloys, *Corros. Sci.* 29 (1989) 899–917. doi:10.1016/0010-938X(89)90060-7.
- [24] E. McCafferty, Graph theory and the passivity of binary alloys, *Corros. Sci.* 42 (2000) 1993–2011. doi:10.1016/S0010-938X(00)00038-X.
- [25] E. McCafferty, Relationship Between Graph Theory and Percolation Approaches in the Passivity of Fe–Cr Binary Alloys, *J. Electrochem. Soc.* 155 (2008) C501. doi:10.1149/1.2958291.
- [26] M. Urquidi, D.D. Macdonald, Solute-vacancy interaction model and the effect of minor alloying elements on the initiation of pitting corrosion, *J. Electrochem. Soc.* 132 (1985) 555–558. doi:10.1149/1.2113886.
- [27] L.F. Lin, C.Y. Chao, D.D. Macdonald, A point defect model for anodic passive films II. Chemical breakdown and pit initiation, *J. Electrochem. Soc.* 128 (1981) 1194–1198. doi:10.1149/1.2127592.
- [28] S. Ogura, K. Sugimoto, Y. Sawada, Effects of Cu, Mo and C on the corrosion of deformed 18Cr8Ni stainless steels in H₂SO₄/NaCl solutions, *Corros. Sci.* 16 (1976) 323–337. doi:10.1016/0010-938X(76)90118-9.
- [29] R.S. Lillard, M.P. Jurinski, J.R. Scully, Crevice Corrosion of Alloy-625 in Chlorinated ASTM Artificial Ocean Water, *Corrosion.* 50 (1994) 251–265. doi:10.5006/1.3294331.
- [30] W. Yang, R.C. Ni, H.Z. Hua, A. Pourbaix, The behavior of chromium and molybdenum in the propagation process of localized corrosion of steels, *Corros. Sci.* 24 (1984) 691–707. doi:10.1016/0010-938X(84)90059-3.
- [31] T. Kodama, J.R. Ambrose, Effect of Molybdate Ion on the Repassivation Kinetics of Iron in Solutions Containing Chloride Ions., *Corrosion.* 33 (1977) 155–161. doi:10.5006/0010-9312-33.5.155.
- [32] J.N. Wanklyn, The role of molybdenum in the crevice corrosion of stainless steels, *Corros. Sci.* 21 (1981) 211–225. doi:10.1016/0010-938X(81)90031-7.
- [33] K. Sugimoto, Y. Sawada, Role of Alloyed Molybdenum in Austenitic Stainless Steels in the Inhibition of Pitting in Neutral Halide Solutions., *Corrosion.* 32 (1976) 347–352.
- [34] M. Urquidi-Macdonald, D.D. Macdonald, S.R.I. International, M. Park, Theoretical Analysis of the Effects of Alloying Elements on Distribution Functions of Passivity Breakdown, 136 (1989).
- [35] J.C. Scully, *The fundamentals of corrosion*, Pergamon Press, 1975. https://books.google.com/books/about/The_fundamentals_of_corrosion.html?id=N7xRAAAAMAAJ (accessed May 31, 2017).
- [36] U.F. Franck, K. Weil, Zur Korrosion des passiven Eisens in Schwefelsäure, *Berichte Der Bunsengesellschaft Für Phys. Chemie.* 56 (1952) 814–822. doi:10.1002/BBPC.19520560825.

7. Further Reading

Books

- Landolt, D. (2007). *Corrosion and surface chemistry of metals*. CRC Press.
- Marcus, P. (2011). *Corrosion mechanisms in theory and practice*. CRC Press.
- Jones, D. A. (1992). *Principles and prevention of corrosion*. Macmillan.

8. Cross References

Passivation and Stainless Steels and other Chromium Bearing Alloys, Corrosion, Surface Analysis, Titanium, Aluminum, Zirconium chapters